



# Size-controlled preparation of $\text{Cu}_2\text{O}$ octahedron nanocrystals and studies on their optical absorption

Ping He, Xinghai Shen\*, Hongcheng Gao

*Department of Applied Chemistry, College of Chemistry and Molecular Engineering, Peking University, Beijing 100871, People's Republic of China*

Received 12 May 2004; accepted 25 October 2004

Available online 16 December 2004

## Abstract

We report herein the size-controlled preparation of monodispersed cuprous oxide octahedron nanocrystals smaller than 100 nm. The method is based on the reduction of copper nitrate in Triton X-100 water-in-oil (w/o) microemulsions by  $\gamma$ -irradiation. The average edge length of the octahedron-shaped nanocrystals varies from 45 to 95 nm as a function of the dose rate. The quantum confinement effect was illustrated by the blueshift in the optical absorption. In addition, the growth process was also traced by absorption spectra.

© 2004 Elsevier Inc. All rights reserved.

*Keywords:* Cuprous oxide; Nanooctahedron;  $\gamma$ -Irradiation; Microemulsion

## 1. Introduction

Cuprous oxide has been the subject of much current research interest, since  $\text{Cu}_2\text{O}$  is an important metal-oxide *p*-type semiconductor and has a direct small band gap of 2.2 eV [1–3], which makes it a promising material for the conversion of solar energy into electrical or chemical energy [4,5]. Recently, its potential was demonstrated by the discovery that illuminated  $\text{Cu}_2\text{O}$  could act as a stable photocatalyst for the photochemical decomposition of water into  $\text{O}_2$  and  $\text{H}_2$  under visible light irradiation [6].

It is well known that the shape and size of inorganic materials have great effects on their widely varying properties [7,8]. So great efforts have been devoted to the synthesis of nanoparticles with various shapes [9–11]. It is noticed that  $\text{Cu}_2\text{O}$  with different shapes has caught much attention [12–20]. Recently, Gou and Murphy [18] reported the solution-phase synthesis of highly monodisperse cubic  $\text{Cu}_2\text{O}$  with cetyltrimethylammonium bromide (CTAB) as the protecting reagent. The dimensions of all the cuprous oxide cubes, however, vary from 200 to 450 nm, much

larger than 100 nm. Submicrosized cuprous oxide octahedra ( $>2 \mu\text{m}$ ) were also prepared by the capping reagent poly(vinylpyrrolidone) (PVP) [13]. Since nanodevices or nanomachines are built of nanometer-sized blocks, the preparation of cuprous oxide nanocrystals with different shapes is of both theoretical and practical importance.

Understanding the growth history is technologically important in the size- and shape-controlled synthesis of nanocrystals and will make it possible to program the system to yield building blocks with desired size and/or shape [19]. In some cases, the optical absorption spectrum is a powerful tool to help us understand the growth history.  $\text{Cu}_2\text{O}$  crystals have high optical absorption coefficient [21] and the size of a crystal can alter the absorption edge greatly [22]. In addition, the bottom of the conduction band and the top of the valence band have the same parity, so that the electric dipole transition between them is forbidden [23]. Quantum size effects on the optical properties of direct band gap semiconductors are phenomenologically different from those on the indirect band gap semiconductors [24,25]. Some works have been focused on the optical absorption of  $\text{Cu}_2\text{O}$  nanocrystals [21,26,27].

The well-dispersed water pool in the w/o microemulsion has been shown to be an ideal nanostructured reaction

\* Corresponding author. Fax: +86-10-62759191.

E-mail address: [xshen@pku.edu.cn](mailto:xshen@pku.edu.cn) (X. Shen).

medium or microreactor, where ultrafine and monodisperse nanoparticles can be formed [28,29]. And the method of  $\gamma$ -irradiation also provides us with a powerful means of preparing nanoparticles different from routine chemical reaction [30,31].

Thus, the research in the present paper is mainly focused on the size-controlled preparation of  $\text{Cu}_2\text{O}$  nanocrystals less than 100 nm in Triton X-100 microemulsions by the  $\gamma$ -irradiation method. Interestingly, the nanocrystals formed mostly have an octahedral shape. Meanwhile,  $\text{Cu}_2\text{O}$  nanocrystals at different stages of formation were explored by the absorption spectra. A blueshift was evidently observed in the optical absorption spectra of  $\text{Cu}_2\text{O}$  nanocrystals of different sizes, which illustrated quantum confinement effects on this direct band gap semiconductor.

## 2. Materials and methods

### 2.1. Materials

Triton X-100 (CP, Beijing Chemical Reagents Inc.), *n*-hexanol (AP, Beijing Kinglong Chemical Products Inc.), cyclohexane, and copper nitrate (AP, Beijing Yili Fine Chemical Products Inc.) were used as received. Deionized and tridistilled water was used in the experiments.

### 2.2. Instruments

All the w/o microemulsions were irradiated in the field of a  $^{60}\text{Co}$   $\gamma$ -ray source. The absorption spectra were recorded by a Hitachi UV-3010 spectrophotometer. TEM images were obtained on a JEM-200CX transmission electron microscope, operating at 120 kV, while HRTEM images were taken on a Hitachi 9000 transmission electron microscope at 300 kV. The stereo shapes of the nanocrystals were explored by a FEI strata dual beam 235 nanoprocessing working station. The powder XRD analysis was performed using a Rigaku Dmax/2400 X-ray diffractometer with graphite monochromatized  $\text{CuK}\alpha$  radiation ( $\lambda = 0.15406$  nm).

### 2.3. Methods

A certain amount of copper nitrate was dissolved in water to obtain a 0.02 mol/L stock solution. To prepare microemulsions, Triton X-100, *n*-hexanol, and cyclohexane (according to the mass ratio Triton X-100/*n*-hexanol/cyclohexane = 4/1/30) were first mixed, and then a certain volume of the stock solution of copper nitrate was added with the molar ratio of water to surfactant fixed at 8.98. The mixtures were stirred mildly at room temperature until they became transparent. Before they were irradiated, the w/o microemulsions were ultrasonicated for 10 min, and bubbled with pure nitrogen for 30 min to remove oxygen.

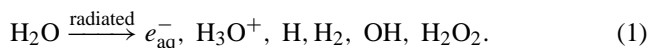
After irradiation, the absorption spectra were recorded immediately with the standard of the identical systems with-

out being irradiated. The irradiated systems were dropped onto a Formvar-covered copper grid placed on filter paper and evaporated in air before characterization by electron microscopy. Before the powder X-ray characterization, the samples were enriched by centrifugation at  $\sim 4000$  rpm, washed by acetone, and deposited on a piece of glass.

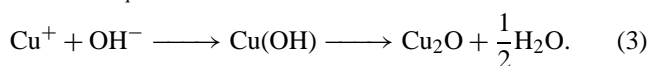
All the experiments were conducted at room temperature.

## 3. Results and discussion

Many products initially generated from the radiolysis of aqueous solutions by  $\gamma$ -rays are well understood:



Some of them have reducing potential, while others have oxidating ability. In the present work, it should be the reducing species, mainly hydrated electrons, that reduce the copper ions to cuprous ions. Then the cuprous ions react with hydroxyl in the system to form cuprous oxide:



A nonnegligible fact, however, is the dismutation of cuprous ions into copper atoms and copper ions. And the cuprous ions can also be reduced further to form copper metal atoms:



It is well known that pH value can have a great effect on the reactions taking place in aqueous systems. Cuprous oxide could be obtained in aqueous systems containing SDS by the  $\gamma$ -irradiation method, when pH was carefully controlled in a small range [32]. If pH were out of this range, the metal phase of copper atoms would appear, mixed with cuprous oxide. In our work, only the cuprous oxide was obtained, using the Triton w/o microemulsion without any pH adjustment of the salt solution in the water pool. In the aqueous solution of SDS, the mechanism of formation of  $\text{Cu}_2\text{O}$  nanoparticles is that the headgroups of many SDS molecules are adsorbed on the surface of a  $\text{Cu}_2\text{O}$  particle to confine its growth. Obviously, the pH will influence the dissociation of SDS and then its adsorption on  $\text{Cu}_2\text{O}$  particles. However, in the w/o microemulsion of Triton X-100, the formation mechanism of the  $\text{Cu}_2\text{O}$  nanoparticles is much different. First, the water pool of the microemulsion provides a real microcompartment or microreactor for the nanoparticles to be formed under the confinement of the surfactant interface. Second, since Triton X-100 is a neutral surfactant, the pH of the water pool does not directly affect the function of Triton X-100. Thus, it is very possible to obtain  $\text{Cu}_2\text{O}$  nanoparticles without adjusting pH.

Fig. 1 illustrates the effect of total dose on the formation of cuprous oxide, when the dose rate is kept at 40.04 Gy/min

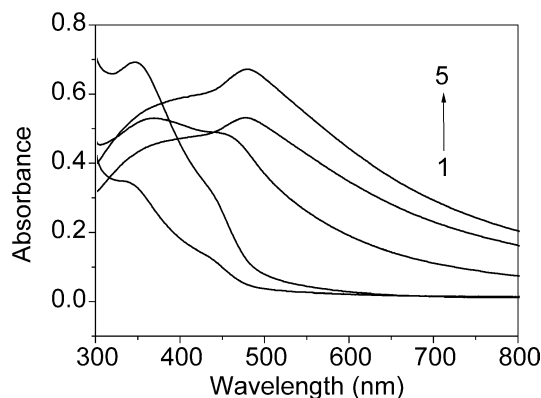


Fig. 1. Evolution of the absorption spectra of 0.02 M  $\text{Cu}(\text{NO}_3)_2$  in the Triton X-100 w/o microemulsion ( $\omega = 8.98$ ) with increasing dose. The dose rate is fixed at 40.04 Gy/min, and yet the irradiation time is changed (from 1 to 5: 10, 20, 24, 30, 40 min).

and the irradiation time is increased. There are mainly two absorptions at  $\sim 338$  nm (peak 1) and  $\sim 465$  nm (peak 2). When the time increases, at first the weak peak 1 becomes stronger, and then turns weaker. Compared with the complex change of peak 1, the situation for peak 2 is relatively simple—it becomes stronger and stronger. As all the absorption spectra show, there is no characteristic absorption of copper metal nanocrystals. Systematic work [22] has illustrated a shift in the absorption towards higher energy with decrease in the size of cuprous oxide nanocrystals. The maximum absorption of  $\text{Cu}_2\text{O}$  nanoclusters having average diameters from  $2.0 \pm 0.5$  to  $45.0 \pm 5.0$  nm shifted from 368 to 584 nm. So we speculate that in our case, first very finite  $\text{Cu}_2\text{O}$  nanoclusters with diameters close to their Bohr excitation radii ( $\sim 7$  Å) are formed, and then due to high surface energy and chemical activity, the small nanoclusters become larger ones by the diffusion mechanism or the aggregation mechanism.

Fig. 2 shows the typical powder X-ray diffraction (XRD) patterns of the as-prepared  $\text{Cu}_2\text{O}$  samples, when the total dose is 20 kGy, and the dose rate is 22.72 Gy/min. Interplanar distances calculated for (110), (111), (200), (220), and (311) from XRD patterns match well with standard data confirming the formation of a single cubic phase  $\text{Cu}_2\text{O}$  with a cuprite structure. No other diffraction peaks arising from metal Cu or CuO appear in the XRD patterns, which is in good agreement with the observations in Fig. 1.

The dose rate also influences the formation of  $\text{Cu}_2\text{O}$  nanoparticles, which is illustrated in Fig. 3. The total dose is chosen at 20 kGy to ensure that all the copper ions are reduced to form cuprous oxide. When the dose rate is largest (curve 1), there is only one obvious absorption at  $\sim 338$  nm and an unobvious shoulder one at  $\sim 450$  nm, which means most of the cuprous oxide is in very tiny form. Then as the dose rate decreases, the absorption at  $\sim 338$  nm becomes weaker and weaker, and yet absorption occurs beyond 440 nm. Carefully studying the spectra of dose rate effect can reveal that the peak of absorption is shifting to lower energy when the dose rate goes down (maximum absorp-

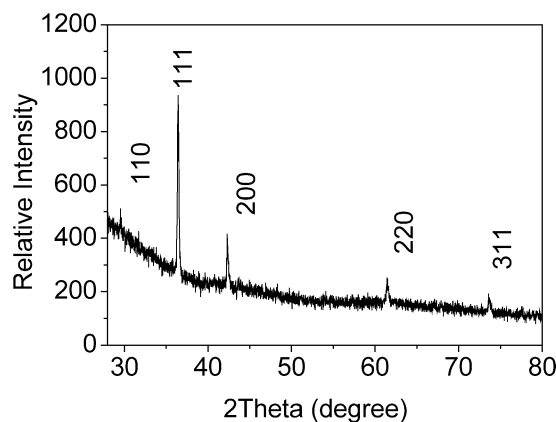


Fig. 2. Powder XRD pattern of  $\text{Cu}_2\text{O}$  nanocrystals of the sample irradiated under a dose rate of 22.72 kGy/min and a total dose of 20 kGy.

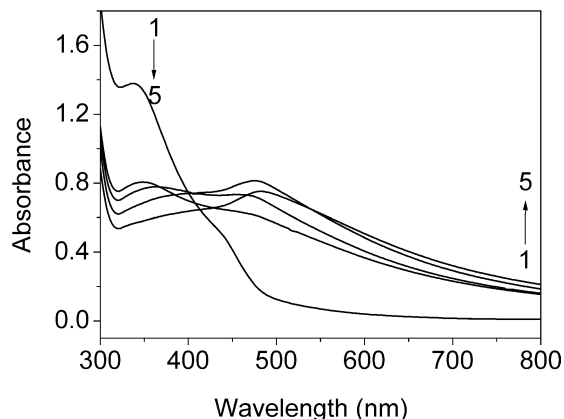


Fig. 3. The dose rate effect on the absorption of the  $\text{Cu}_2\text{O}$  nanoparticles. The total dose is fixed at 20 kGy, while the dose rate is different (from 1 to 5: 131.95, 92.24, 75.57, 40.04, 22.72 Gy/min).

tion from 460 nm to 482 nm). According to the systematic study [22] on the blue shift with the decreasing size of  $\text{Cu}_2\text{O}$  nanocrystals, we speculate that the size of  $\text{Cu}_2\text{O}$  nanocrystals in our case could be controlled by applying a different dose rate to the system.

To substantiate our speculation, the morphologies of the samples studied in Fig. 3 were characterized by transmission electron microscopy (TEM) as shown in Fig. 4. By comparison of the nanocrystal sizes, the effect of dose rate on the formation of  $\text{Cu}_2\text{O}$  nanoparticles is confirmed: the higher the dose rate, the smaller the nanoparticles. When the dose rate is highest, only rounded nanoparticles of  $\sim 3$  nm but no other shaped nanoparticles can be seen (1A and 1B in Fig. 4). Most  $\text{Cu}_2\text{O}$  square-shaped nanocrystals with edge length  $45 \pm 5$ ,  $55 \pm 5$ ,  $65 \pm 5$ ,  $95 \pm 10$  nm can be seen from Fig. 4(2) to Fig. 4(5), respectively. Even the superlattice of the self-assembly of nanoparticles due to the small distribution of the nanoparticles can be seen in Fig. 4(3). The relationship between the dose rate and the size of the  $\text{Cu}_2\text{O}$  nanoparticle can be seen clearly from Fig. 5. It should be pointed out here that the absorption wavelength of about 482 nm for the  $\text{Cu}_2\text{O}$  nanoparticle with diameter 95 nm seems not to agree

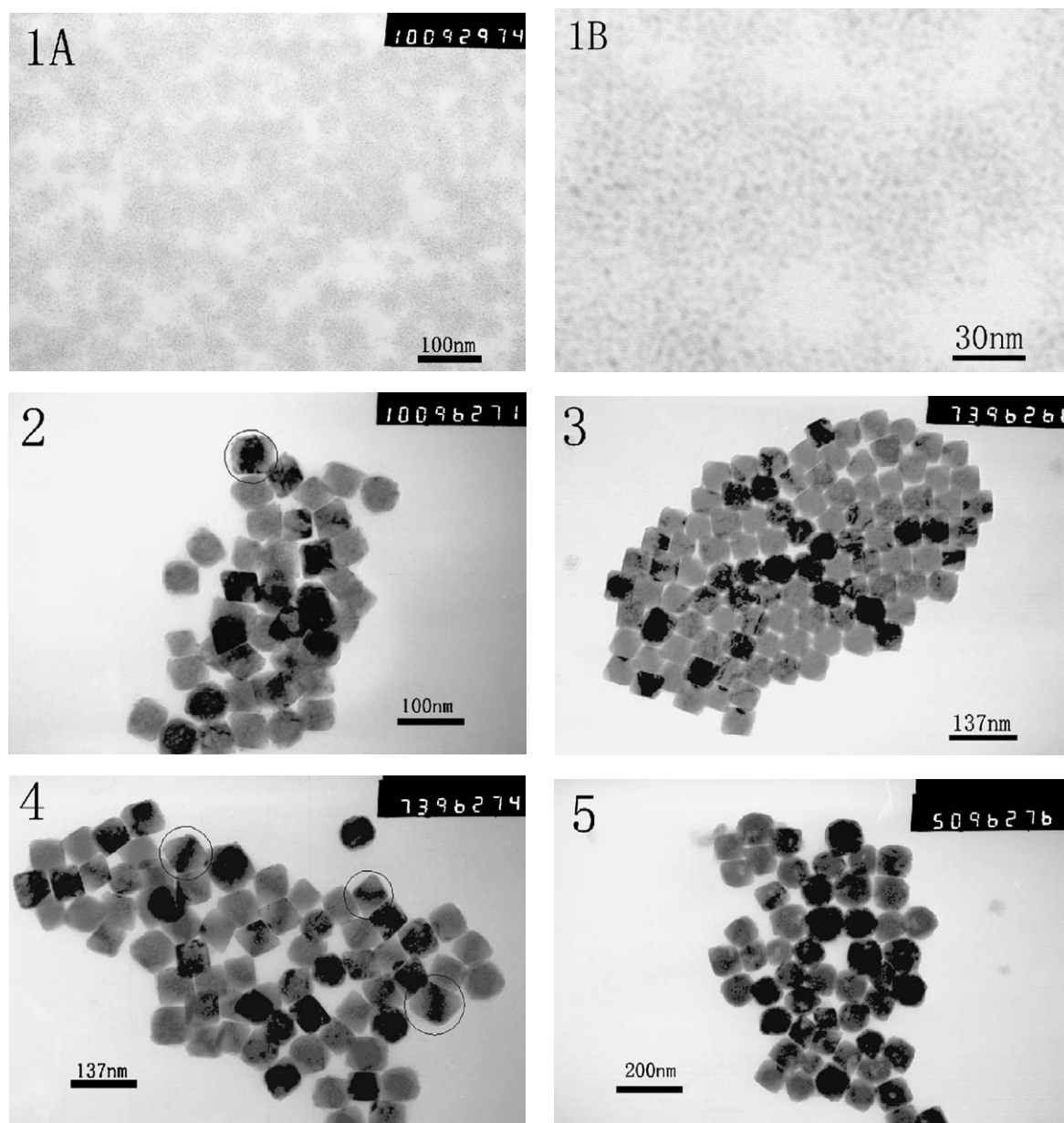


Fig. 4. Micrographs of  $\text{Cu}_2\text{O}$  nanoparticles of the same samples studied in Fig. 3.

well with that in the literature [22], where the reported absorption wavelength for  $\text{Cu}_2\text{O}$  nanoparticles with diameter of 45 nm is 584 nm. Two reasons can be used to explain the discrepancy. First, the shape of inorganic nanoparticles may cast great influence on their properties. It is postulated here that the special octahedrons of  $\text{Cu}_2\text{O}$  nanoparticles have different properties from the round-shaped ones. Second, the absorption of nanoparticles or nanoclusters can be changed greatly by the media surrounding them. For instance,  $\text{Ag}_2$  nanoclusters absorb light at the wavelengths of 331, 271, 310, and 476 nm in Nr, Kr, aqueous solution, and photo latex, respectively [33].

As illustrated by a typical high-resolution transmission electron microscopy (HRTEM) image of a nanocrystal in Fig. 6, the visible lattice fringes in this image show that

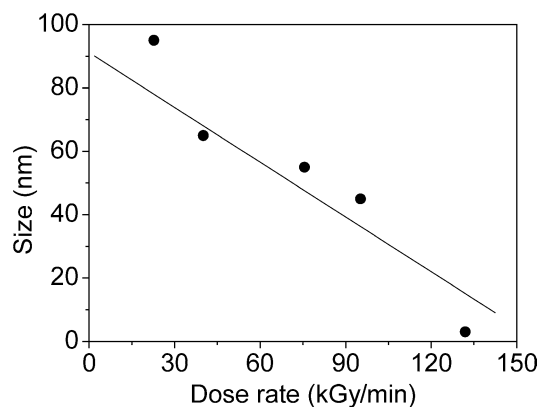


Fig. 5. The relationship between the dose rate and the size of the  $\text{Cu}_2\text{O}$  nanoparticles studied in Figs. 3 and 4.

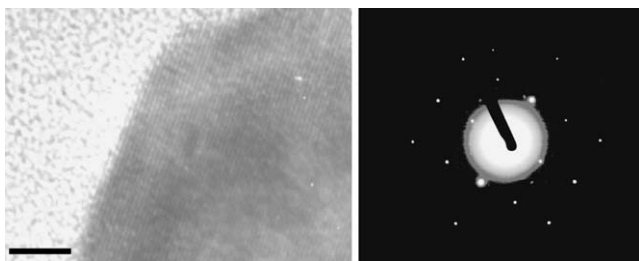


Fig. 6. HRTEM (left) and SAED (right) images of an individual  $\text{Cu}_2\text{O}$  nanooctahedron of sample 5 studied in Fig. 3. The scale bar is 35.8 Å.

the nanoparticle is a single crystal. The interplanar spacing is about 2.468 Å, corresponding to the {111} plane of cubic  $\text{Cu}_2\text{O}$ . But the selected area electron diffraction (SAED) in ordinary TEM demonstrates the smallest cuprous oxide nanoparticles are the mixture of polycrystals and monocrystals (see Fig. 4(1A)). The formation of the single crystal phase of the  $\text{Cu}_2\text{O}$  nanocrystals can also be confirmed.

A puzzle is why there is difference in the grayness for the different nanocrystals, and even in a single crystal. Different grayness of the different part of a single crystal can be clearly seen in the nanoparticles marked with circle (see Figs. 4(2) and 4(4)); that is, the equatorial part is darker than the polar part. So we speculate that the nanocrystals are neither square nor cubic, for TEM images can only provide projected shape information on the samples, no matter what the real shapes of the samples are in three dimensions. Scanning electron microscopy (SEM) can help us know the exact shape of samples. From the SEM images in Fig. 7, it can be seen clearly that the nanocrystals are actually octahedra, which confirms our speculation. The difference of the grayness in the TEM images can be explained in terms of the different orientations of octahedron nanocrystals and the different thickness in a single octahedral nanocrystal.

As is well known, two completely different mechanisms are usually used to explain the formation of single crystals and polycrystals. A diffuse mechanism originally suggested by Lamer [34,35] is now generally accepted to explain the formation of monodispersed single crystals. According to this scheme, the precipitation process begins with a short burst of nuclei once critical supersaturation of the particle-forming species is reached. The nucleation stage is then followed by diffusion of the constituent complexes to these primary particles until the supply is exhausted. On the other hand, the aggregation mechanism [36–40] could be used to explain the formation of monodisperse polycrystals. This mechanism indicates that uniform particles formation usually proceeds in several stages. In the initial induction stage, solutes are formed to yield a supersaturated solution, leading to nucleation. The nuclei then grow by diffusive mechanism to form crystalline subunits, which in turn aggregate to form the large polycrystalline assemblages.

Differences in two mechanisms have been discussed recently. These two mechanisms are believed to coexist, influencing the morphologies of the  $\text{Cu}_2\text{O}$  particles under

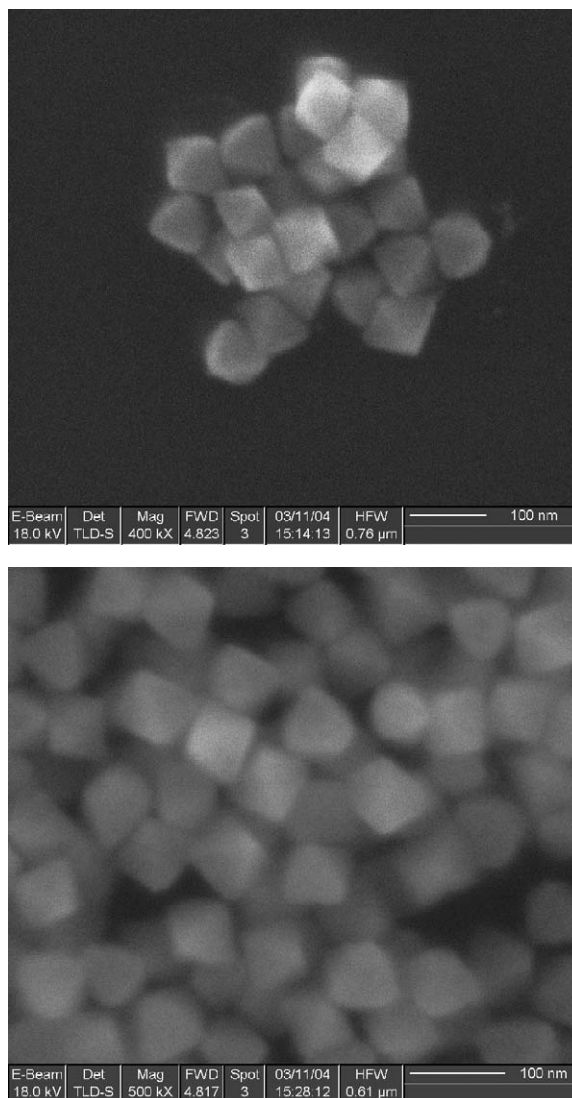


Fig. 7. SEM images and schemes of sample 2 studied in Fig. 3.

competitive condition [17]. In other words, the nucleation process is accompanied by diffusion as well as aggregation. Competition between the two mechanisms is believed to exist in our work. As discussed above, the cuprous oxide is derived from copper ion reduced by hydrated electrons. And all the experiment conditions are identical to each other except the dose rate. So it is speculated that when the dose rate is high, the aggregation mechanism overwhelms the diffusion mechanism, so  $\text{Cu}_2\text{O}$  forms mainly polycrystals; in contrast, when the dose rate becomes lower, the  $\text{Cu}_2\text{O}$  single crystals are formed.

#### 4. Conclusion

$\text{Cu}_2\text{O}$  octahedral nanocrystals smaller than 100 nm have been prepared successfully in Triton X-100 w/o microemulsions using the  $\gamma$ -irradiation method. And the size of the nanocrystals could be controlled by the dose rate. The ab-

sorption spectra have been applied to explore the quantum confinement effect of the semiconductor, in which an evident blueshift of the absorption was observed. And it was suggested that competition between the diffusion mechanism and the aggregation mechanism occurred in our case. In addition, the growth process was also traced by the absorption spectra, demonstrating that at the selected dose rate, small Cu<sub>2</sub>O nanoparticles were formed first, then larger nanocrystals.

## Acknowledgments

This work was supported by the Natural Science Foundation of China (Grants 90206020, 29901001). Sincere thanks are due to Jun Xu, Yuping Wang, and Xiuzheng Gai in the Electron Microscopy Laboratory, Peking University, for help with SEM and TEM experiments and to Deliang Sun for assistance in the  $\gamma$ -irradiation experiments.

## References

- [1] I. Grozdanov, *Mater. Lett.* 19 (1994) 281.
- [2] M.Y. Shen, T. Yokouchi, S. Koyama, T. Goto, *Phys. Rev. B* 56 (1997) 13066.
- [3] W. Shi, K. Lim, X. Liu, *J. Appl. Phys.* 81 (1997) 2822.
- [4] R.N. Briskman, *Sol. Energy Mater. Sol. Cells* 27 (1992) 361.
- [5] L.C. Olsen, F.W. Addis, W. Miller, *Sol. Cells* 7 (1982) 247.
- [6] M. Hara, T. Kondo, M. Komoda, S. Ikeda, K. Shinohara, A. Tanaka, J.N. Kondo, K. Domen, *Chem. Commun.* (1998) 357.
- [7] A.P. Alivisatos, *Science* 271 (1996) 933.
- [8] M.A. El-Sayed, *Acc. Chem. Res.* 34 (2001) 257.
- [9] Y.G. Sun, Y.N. Xia, *Science* 298 (2002) 2176.
- [10] Z.L. Wang, *J. Phys. Chem. B* 104 (2000) 1153.
- [11] M. Jose-Yacama, J.A. Ascencio, H.B. Liu, J. Gardea-Torresdey, *J. Vac. Sci. Technol. B* 19 (2001) 1091.
- [12] D.B. Wang, M.S. Mo, D.B. Yu, L.Q. Xu, F.Q. Li, Y.T. Qian, *Cryst. Growth Des.* 3 (2003) 717.
- [13] X. Zhang, Y. Xie, F. Xu, X.H. Liu, D. Xu, *Inorg. Chem. Commun.* 6 (2003) 1390.
- [14] Z. Chen, E. Shi, Y. Zheng, W. Li, B. Xiao, J. Zhuang, *J. Cryst. Growth* 249 (2003) 294.
- [15] W.Z. Wang, G.H. Wang, X.S. Wang, Y.J. Zhan, Y.K. Liu, C.L. Zheng, *Adv. Mater.* 14 (2002) 67.
- [16] S.J. Chen, X.T. Chen, Z.L. Xue, L.H. Li, X.Z. You, *J. Cryst. Growth* 246 (2002) 169.
- [17] Y.J. Dong, Y.D. Li, C. Wang, A.L. Cui, Z.X. Deng, *J. Colloid Interface Sci.* 243 (2001) 85.
- [18] L.F. Gou, C.J. Murphy, *Nano Lett.* 3 (2003) 231.
- [19] S.M. Lee, S.N. Cho, J. Cheon, *Adv. Mater.* 15 (2003) 441.
- [20] D.B. Wang, D.B. Yu, M.S. Mo, X.M. Liu, Y.T. Qian, *J. Colloid Interface Sci.* 261 (2003) 565.
- [21] A.O. Musa, T. Akomolafe, M.J. Carter, *Sol. Energy Mater. Sol. Cells* 51 (1998) 305.
- [22] K. Borgohain, N. Murase, S.J. Mahamuni, *Appl. Phys.* 92 (2002) 1292.
- [23] R.J. Elliot, *Phys. Rev.* 124 (1961) 340.
- [24] T. Masumoto, J.-I. Sujuki, M. Ohnuma, Y. Kanemitsu, Y. Masumoto, *Phys. Rev. B* 63 (2001) 195322.
- [25] S.S. Lyer, Y.H. Xie, *Science* 264 (1993) 40.
- [26] S. Banerjee, D. Chakravorty, *Europhys. Lett.* 52 (2000) 468.
- [27] S. Deki, K. Akamatsu, T. Yano, M. Mizuhata, A. Kajinami, *J. Mater. Chem.* 8 (1998) 1865.
- [28] V. Pillai, P. Kumar, M.J. Hou, P. Ayyub, D.O. Shah, *Adv. Colloid Interface Sci.* 55 (1995) 241.
- [29] M.P. Pileni, *J. Phys. Chem.* 97 (1993) 6961.
- [30] J. Belloni, M. Mostafavi, H. Remita, J.-L. Marignier, M.-O. Delcourt, *New J. Chem.* 22 (1998) 1239.
- [31] A. Henglein, *J. Phys. Chem.* 97 (1993) 5457.
- [32] Y.J. Zhu, Y.T. Qian, M.W. Zhang, Z.Y. Chen, D.F. Xu, *Mater. Res. Bull.* 29 (1994) 377.
- [33] B.X. Peng, W.D. Cui, X. Zhao, *Prog. Chem.* 10 (1998) 362.
- [34] V.K. Lamer, R.H. Dinegar, *J. Am. Chem. Soc.* 72 (1950) 4847.
- [35] V.K. Lamer, *Ind. Eng. Chem.* 44 (1952) 1270.
- [36] W.P. Hsu, L. Ronnquist, E. Matijevic, *Langmuir* 14 (1998) 38.
- [37] M. Ocana, E. Matijevic, *J. Mater. Res.* 5 (1990) 1083.
- [38] M. Ocanal, R. Rodriguez-Clemente, C.J. Serna, *Adv. Mater.* 7 (1995) 212.
- [39] S.H. Lee, Y.S. Her, E. Matijevic, *J. Colloid Interface Sci.* 186 (1997) 193.
- [40] V. Privman, D.V. Goia, J. Park, E. Matijevic, *J. Colloid Interface Sci.* 213 (1999) 36.